

# ASSESSMENT OF CO<sub>2</sub> FLUXES IN THE DRY GRASSLAND OF SOUTHERN WESTERN SIBERIA

A. A. Bondarovich\*<sup>1</sup>, D. V. Ilyasov<sup>2</sup>, A. A. Kaverin<sup>2</sup>, D.W. Kirillov<sup>1</sup>, E.Yu. Mordvin<sup>1</sup>, Artemy I.  
Revyakin<sup>1</sup>, A. A. Shibanova<sup>1</sup>, T.M. Kopytina<sup>1</sup>

<sup>1</sup>*Altai State University, pr. Lenina 61, 656049, Barnaul, Russian Federation*

<sup>2</sup>*Yugra State University, ul. Chekhova 16, 628012, Khanty-Mansiysk, Russian Federation*

\* **Corresponding author:** bondarovich@geo.asu.ru

**Abstract.** For the first time, net ecosystem exchange (NEE) and ecosystem respiration ( $R_{eco}$ ) were measured using the chamber method within the dry grassland (true steppe) of the Kulunda Plain, West Siberia, (Altai Krai), and gross primary production (GPP) was calculated. To identify the relationship between CO<sub>2</sub> fluxes and environmental factors, the following parameters were also measured: aboveground phytomass (AGP), photosynthetically active radiation (PAR), air temperature, soil temperature and soil moisture. The median (1Q, 3Q) NEE,  $R_{eco}$ , and GPP were -103 (-152, -66), 90 (74, 105), and -200 (-251, -151) mg C m<sup>-2</sup> h<sup>-1</sup>, respectively. The key factors of variability in NEE and GPP were aboveground phytomass, while for  $R_{eco}$  – soil moisture content in the 100 cm layer. Based on the obtained data, a neural network was successfully trained using the Levenberg-Marquardt algorithm ( $R^2_{train} = 0.9$ ,  $R^2_{valid} = 0.9$ ,  $R^2_{test} = 0.8$ ;  $MSE_{train} = 335$ ,  $MSE_{valid} = 647$ ,  $MSE_{test} = 360$ ;  $N_{train} = 50$ ;  $N_{train} = 11$ ), which will be used in the future to scale carbon fluxes in space and time.

**Key Words:** carbon dioxide, summer fluxes, dry grassland, regional natural monument, south of Western Siberia, Kulunda Plain, Altai Krai.

## Acknowledgements

*This work was supported by the Ministry of Science and Higher Education of the Russian Federation as a State Assignment for scientific research carried out at Altai State University, project FZMW-2023-0007.*

## ОЦЕНКА ПОТОКОВ СО<sub>2</sub> В НАСТОЯЩЕЙ СТЕПИ ЮГА ЗАПАДНОЙ СИБИРИ

А.А. Бондарович\*<sup>1</sup>, Д.В. Ильясов<sup>2</sup>, А.А. Каверин<sup>2</sup>, Д.В. Лагутин<sup>1</sup>, Е.Ю. Мордвин<sup>1</sup>, А. И.  
Ревякин<sup>1</sup>, Шибанова А.А.<sup>1</sup>, Копытина Т. М.<sup>1</sup>

<sup>1</sup>*Алтайский государственный университет, просп. Ленина, 61, 656049, Барнаул, Российская Федерация*

34 <sup>2</sup> Югорский государственный университет, ул. Чехова, 16, 628012, Ханты-Мансийск, Российская  
35 Федерация

36 \* Автор для переписки: bondarovich@geo.asu.ru

37 **Аннотация.** Впервые в пределах настоящей степи Кулундинской равнины, Западная  
38 Сибирь (Алтайский край) камерным методом были измерены чистый экосистемный обмен  
39 (NEE) и экосистемное дыхание (Resc), а также рассчитана валовая первичная продукция  
40 (GPP). Для выявления связи потоков CO<sub>2</sub> с факторами среды также измерялись следующие  
41 параметры: надземная фитомасса (AGP), фотосинтетически активная радиация (ФАР),  
42 температура воздуха, температура почвы и ее влажность. Медианные (1Q, 3Q) значения  
43 NEE, Resc и GPP составили -103 (-152, -66), 90 (74, 105) и -200 (-251, -151) мг С м<sup>-2</sup> ч<sup>-1</sup>  
44 соответственно. Ключевыми факторами изменчивости NEE и GPP были надземная  
45 фитомасса, а для Resc – влажность почвы в слое 100 см. На основе полученных данных  
46 успешно обучена нейронная сеть с использованием алгоритма Левенберга-Марквардта  
47 (R<sub>2</sub>train = 0,9, R<sub>2</sub>valid = 0,9, R<sub>2</sub>test = 0,8; MSEtrain = 335, MSEvalid = 647, MSEtest = 360;  
48 Ntrain = 50; Ntrain = 11), которая в дальнейшем будет использоваться для масштабирования  
49 потоков углерода в пространстве и времени.

50 **Ключевые слова:** углекислый газ, летние потоки, настоящие степи, памятник природы,  
51 юг Западной Сибири, Кулундинская равнина, Алтайский край.

52

53 **Благодарности.** Работа выполнена при поддержке Министерства науки и высшего  
54 образования Российской Федерации в рамках государственного задания на научно-  
55 исследовательскую работу, выполняемую в Алтайском государственном университете,  
56 проект FZMW-2023-0007.

57

## 58 **Introduction**

59 Finding ways to adapt to climate change requires refining regional estimates of the CO<sub>2</sub> (and  
60 other greenhouse gas) balance (Cenci and Biffis 2025), which has been identified as a global  
61 priority at the national (Decree... 2020; Strategy... 2021) and international levels (IPCC 2023).

62 Inventorying and long-term forecasting of the CO<sub>2</sub> balance is typically carried out using  
63 mathematical simulation methods, which requires validation using regional field data.  
64 Furthermore, it is important not only to measure CO<sub>2</sub> fluxes at different spatial scales and types of  
65 terrestrial ecosystems, but also to explore and analyze their complex relationships with  
66 meteorological and environmental factors (Pillai et al. 2025). The most important of these are soil

67 temperature and moisture, as well as the input of substrates from plants into soil biota (Hu et al.  
68 2024). Also, the CO<sub>2</sub> balance of a particular ecosystem depends on local environmental conditions  
69 and land use types (Li et al. 2020; Wang and Ma 2022; Wang et al. 2024). For example, in  
70 waterlogged alpine meadows, CO<sub>2</sub> fluxes are mainly controlled by soil temperature, while in water-  
71 deficient steppe ecosystems, they are controlled by soil moisture in the root zone (Wang and Ma  
72 2022). In international practice, studies on measuring CO<sub>2</sub> fluxes have been carried out mainly in  
73 forest and wetland ecosystems (Mazzola et al. 2021; Shokoufeh et al. 2021), while in the steppes  
74 such measurements are rare (Gilmanov et al. 2003; Perez-Quezada et al. 2010, Zhang et al. 2007;  
75 Wen et al. 2024). A detailed review of balance estimates of net ecosystem production (NEP) of  
76 CO<sub>2</sub> in the steppe zone of the world based on instrumental measurements from 1997 to 2011 is  
77 presented in the paper by (Golubyatnikov et al. 2023). In Russia, there is also a prevailing interest in  
78 taiga forest and wetland ecosystems, where measurements are mainly organized using the Eddy  
79 covariance (EC) method (Glagolev 2010; Monitoring..., 2017; Kazantsev et al. 2018; Mamkin et  
80 al. 2019; Dyukarev et al. 2019; Kuricheva et al. 2023). This is partly due to the fact that forests  
81 account for 61% of Russia's total ecosystem area, tundra for 18%, swamps for 10%, and grassland  
82 ecosystems for 6%. Preserved and restored steppe ecosystems account for only 3.4%, with only 1%  
83 conserved in protected areas (Assessment... 2023, p. 56). In the Altai Krai, natural steppes account  
84 for 2.9%, and restored steppes account for 7% of the region's total area. (Assessment... 2023, p. 63).  
85 Moreover, the steppes are a critical component of biodiversity and are characterized by the largest  
86 soil carbon reserves in southern Russia.

87 A limited number of model estimates of net primary production (NPP) and ecosystem  
88 respiration ( $R_{\text{eco}}$ ) have been obtained for steppe ecosystems in Russia (Titlyanova and Shibareva  
89 2017; Assessment... 2023). These data are comparable with the same assessments of CO<sub>2</sub>: NPP for  
90 steppe ecosystems in Russia (Golubyatnikov et al. 2023). However, these model estimates require  
91 refinement to ensure a reliable accounting of steppe area, as well as the use of a broader set of  
92 factual data for validation (Assessments... 2023). Among the instrumental measurements in the  
93 steppes, it is also worth noting the net ecosystem exchange (NEE) estimates using the EC method  
94 (natural background and fallow) in the Republic of Khakassia (Belelli Marchesini et al. 2007,  
95 Vuichard et al. 2008). Noteworthy are the  $R_{\text{eco}}$  estimates obtained using the EC method on the East  
96 European Plain within forest-steppe agroecosystems, mixed and broad-leaved forests during 2020–  
97 2022 growing seasons (Sukhoveeva et al. 2023). This confirms that direct instrumental ground-  
98 based measurements of CO<sub>2</sub> fluxes in steppe ecosystems in Russia are currently few and have not  
99 been conducted in the Altai Krai.

100 It should also be emphasized that greenhouse gas (GHG) emission datasets are often  
101 incomplete due to inconsistent reporting and difficulties in organizing ground-based observations,  
102 and recently there has been an increasing number of studies on filling these gaps and, in general, on  
103 estimating carbon emissions based on machine learning (Cullen et al. 2024; Feng et al. 2024; Al  
104 Nuaimi et al. 2025). Satellite remote sensing data (MODIS/Terra) for grass communities (Zhukov  
105 and Zhukova 2023) and forest ecosystems (Rygalova et al. 2024) are also actively and successfully  
106 used to estimate GHG fluxes in the absence of ground-based measurements. In this regard, the  
107 purpose of this study is to evaluate CO<sub>2</sub> fluxes using static cameras and test machine learning  
108 methods for scaling CO<sub>2</sub> fluxes in space and time in conditions of a shortage (short series) of  
109 instrumental observations of fluxes and using only climatic parameters, which are usually easier to  
110 organize and long-term. To achieve this goal, ground-based instrumental measurements of CO<sub>2</sub>  
111 fluxes and related environmental factors were carried out for the first time in the arid meadows of  
112 the Altai Territory. The neural network was trained using short series data obtained using the  
113 Levenberg-Marquardt algorithm.

## 114 **Materials and methods**

### 115 **Study Area**

116 Measurements of CO<sub>2</sub> fluxes and associated environmental factors were carried out from July  
117 22 to 25, 2024, at four measurement sites (MS) on the territory of the regional natural monument  
118 “Balochnaya system in Novokormikha” (protected area since May 6, 2014), located on the Kulunda  
119 Plain in the Altai Krai ( coordinates: 52.143755, 80.086703, WGS84). (Balochnaya system...  
120 2025).

121

### 122 **Climate and Weather Conditions**

123 According to data from the nearest Roshydromet weather station, Volchikha (located 30 km  
124 southeast of the study site), average annual air temperatures from 1995 to 2024 ranged from 0.5 to  
125 4.5°C, while precipitation over the same period ranged from 190 mm to 580 mm. In 2024, the  
126 average annual temperature was 4°C, and precipitation was approximately 400 mm, indicating  
127 warm and moist conditions during the measurement period. Over the past 5 years, the 2024 growing  
128 season was the most humid, but not the hottest, while the period from June to August was  
129 characterized by the highest average daily air temperatures. During the field work itself, rain was  
130 observed on July 22 (night and day), and also on the night of July 25.

### 131 **Vegetation and Soils**

132 The natural monument is a gully up to 15 m deep and overgrown with birch forest, and an  
 133 adjacent flat area. The southwestern aspect of the gully is covered with steppe vegetation, and the  
 134 northeastern one is covered with a community with a tree layer (*Betula pendula*). The bottom of the  
 135 gully is composed of complexes of meadow and hydrophytic vegetation. The vegetation of the  
 136 study area belongs to the class of dry grassland formations (Lavrenko 1940, 1991; Ronginskaya  
 137 1963). Measurements of flows, environmental factors, and botanical descriptions were carried out  
 138 on the flat area, where forb-feather-grass dry grassland grows on low-humus, medium-deep  
 139 southern chernozems, classified as Chernozem according to the FAO classification, and Calcic,  
 140 Chca according to the WRB classification (Balochnaya system... 2025). During field geobotanical  
 141 releves, two steppe communities were identified, named according to the dominant species of the  
 142 identified sublayers. The communities are located 20 meters apart. The geobotanical releves were  
 143 prepared using generally accepted methods and processed using the dominant-determinate system.  
 144 They contain the following phytocoenotic data: phenological indices of dominant species, floristic  
 145 diversity of communities, and total projective cover (PC). The dominants within each MS were  
 146 identified. Latin plant names are given according to the International Plant Names Index (IPNI  
 147 2025). Four MS were established in the territory of these communities to measure CO<sub>2</sub> fluxes (Fig.  
 148 1).



150 Fig.1. CO<sub>2</sub> flux measurement sites. MS 1–4 are marked as T 1–4, respectively. MS 1 and 4 are  
 151 feather-grass wormwood steppe, MS 2 and 3 are fescue-feather-grass steppe  
 152

### 153 Aboveground Phytomass

154 AGP was mown within each measurement site. Phytomass reserve (P) was calculated using the  
 155 formula:

$$156 P = AGP_{raw} - AGP_{dry} / S_{MS}, (1)$$

157 where  $AGP_{raw}$  – weight of raw AGP in grams,  $AGP_{dry}$  – weight of dried AGP in grams,  $S_{MS}$  – area  
158 of measurement site in  $m^2$ . Drying was carried out in a drying chamber at a temperature of  $105^\circ C$   
159 until an absolutely dry state was achieved.

### 160 **CO<sub>2</sub> Flux Measurements**

161 CO<sub>2</sub> fluxes were measured using the static chamber method using transparent and opaque  
162 chambers (closed with covers made of foil-clad polyethylene foam, which additionally reduced  
163 their heating). Transparent chambers were used to measure CO<sub>2</sub> fluxes: NEE, and opaque ones – for  
164  $R_{eco}$ . GPP was calculated as the difference between NEE and  $R_{eco}$  (with negative values  
165 corresponding to the CO<sub>2</sub> sink from the atmosphere to ecosystems and vice versa). The chambers  
166 were made of transparent 4 mm thick organic glass in the shape of a parallelepiped (height – 70 cm,  
167 side dimensions –  $34 \times 34$  cm, volume –  $0.103 m^3$ ) (Fig. 2). The chambers were equipped with  
168 samplers with silicone hoses. Settled well water was poured into a trough at the base, functioning as  
169 a water seal. The air in the chambers was mixed with a fan with an air flow rate of  $0.88 m^3/min$ . To  
170 reduce the impact of the foundation insertion on the soil gas profile, they were installed on July 22,  
171 2024, 12 hours before the start of measurements. A portable infrared gas analyzer EGM-5 Portable  
172 CO<sub>2</sub> Gas Analyzer (PP-System, USA) with a concentration measurement error of  $<1\%$  was used to  
173 measure the concentration of carbon dioxide over a range of  $0-100,000$  ppm. Measurements were  
174 carried out at each MS in triplicate in the morning from 9:30 to 11:30 am and in the evening from  
175 4:00 to 6:00 pm. The exposure duration was 3 minutes. Specific CO<sub>2</sub> fluxes were calculated in the  
176 MatLab software package (MathWorks, Inc., USA) using the formula:

$$177 \quad flux = 2 a P M b \frac{H}{T + T_0}, \quad (2)$$

178 where  $flux$  – specific CO<sub>2</sub> flux ( $mg C m^{-2} h^{-1}$ ),  $a = 0.12 mg mol K / (kg J ppm)$ ,  $P$  – total pressure of  
179 the gas mixture (Pa),  $M$  – molar mass of gas ( $0.012 kg/mol$  for express flux in  $mg C m^{-2} h^{-1}$ ),  $b$  – the  
180 rate of change of gas concentration in the chamber atmosphere (ppm/h; calculated as the slope of  
181 the line representing the increase in gas concentration in the chamber using the least squares method  
182 with weights, fitlm function, MATLAB),  $H$  – chamber height (m),  $T$  – temperature in the chamber  
183 at the end of the measurement (K),  $T_0$  – temperature in the chamber at the beginning of the  
184 measurement (K).

185 Absolute error of flux was estimated using the formula:

$$186 \quad \Delta flux = 2 a P M \frac{1}{T + T_0} (\Delta b H + |b| \Delta H). \quad (3)$$

187 Here  $\Delta b$  – error in determining the parameter  $b$  (ppm/h),  $\Delta H$  – is the error in determining the  
188 camera height (m; assumed to be 0.05 m, which is mainly due to the inaccuracy of estimating the  
189 camera installation height due to surface unevenness). To compare the obtained instrumental  
190 estimates of GPP and NPP, the satellite remote sensing product MOD17A2HGF.061 (Terra Gross  
191 Primary Productivity), which is an 8-day composite with a 500-meter spatial resolution of GPP  
192 values (Running and Zhao 2021).

### 193 **Ecological Factors**

194 For continuous monitoring of air and soil temperature during daylight hours, autonomous  
195 ThermoChron iButton DS1921 sensors (Dallas Semiconductor, USA) were installed at a height of  
196 100 cm and a depth of 0.30 cm. They were set to measure at a frequency of 3 hours and had an  
197 accuracy of  $\pm 0.5^\circ\text{C}$ . In the immediate vicinity of each MS, soil volumetric moisture content was  
198 measured in percentages at the surface once daily from 13:00 to 16:00 and then in 10 cm increments  
199 down to a depth of 100 cm using an express kit consisting of an NN-2 data logger and an ML3  
200 ThetaProbe sensor (measurement accuracy of  $\pm 1\%$ ) (Delta-T Devices, UK). The total solar  
201 radiation (TSR) intensity was measured during daylight hours using a Janiszewski thermoelectric  
202 pyranometer connected to an EMS12 data recorder (Environmental Measuring Systems, Czech  
203 Republic), with continuous data recording during daylight hours at a frequency of 20 times/min.  
204 The measurement period was predominantly cloudless, so uniform conversion factors were used  
205 first from volts to  $\text{kcal}/\text{cm}^2 \text{min}$  (calibration coefficient – 0.12), and then to  $\text{W}/\text{m}^2$  (coefficient – 698)  
206 (Photosynthesis... 1989).

### 207 **Statistical data processing and machine learning**

208 Standard nonparametric statistics were calculated for the obtained data: the sample median for  
209  $\text{CO}_2$  flux measurements and environmental factors, and uncertainty characteristics – the first and  
210 third quartiles. Statistical hypotheses were tested using the Kruskal-Wallis test at a significance  
211 level of  $p=0.01$ . The model (input: environmental factors; output:  $\text{CO}_2$  fluxes) was developed  
212 using machine learning using the Neural Network Toolbox module in MATLAB. A standard two-  
213 layer feed-forward NN was used. The Levenberg-Marquardt algorithm was used for NN training, as  
214 it is the most universal method suitable for most problems. Furthermore, it has proven effective  
215 when working with small training sets and weak correlations between  $\text{CO}_2$  fluxes and  
216 environmental parameters (Beale et al. 2010). The input parameters were checked for high internal  
217 correlation ( $R^2 \geq 0.5$ ) using the correlation matrix. The original set of input and target data was  
218 divided (by default) into three subsets: the training subset “Training” (70%), which was used to  
219 adjust the neural network weights by minimizing the model error (Beale et al. 2010); the test subset

220 “Testing” (15%), which was used to independently evaluate the performance of the trained model;  
 221 and the validation subset “Validation” (15%), which was used to monitor training and stop testing if  
 222 there was no improvement. The number of layers of neurons (10) in the hidden subset was selected  
 223 empirically to achieve the highest training efficiency, which was expressed by the lowest MSE  
 224 (Beale et al. 2010).

225

## 226 **Results and discussion**

227 During the fieldwork, geobotanical relevés of the steppe communities and the measurement  
 228 sites established within them were conducted. MS1 and MS4 were established in feather-grass-  
 229 wormwood steppe communities: *Stipa capillata*, *Artemisia frigida*, *Festuca pseudovina*, *Koeleria*  
 230 *pyramidata* (Fig. 2) MS2 and MS3 were established in fescue-feather-grass-steppe communities:  
 231 *Stipa capillata*, *Festuca pseudovina* (Fig. 2). AGP was calculated at each MS (see Table 2).

232 As a result of measurements at the MS, data were obtained on NEE and R<sub>eco</sub>: CO<sub>2</sub>, as well as  
 233 associated environmental factors: air temperature at a height of 100 cm, PAR, soil temperature at  
 234 the surface and at a depth of 30 cm, and volumetric soil moisture in a 100-cm layer with  
 235 measurements every 10 cm. Based on these measurements, GPP: CO<sub>2</sub> was calculated. The results of  
 236 all measurements are presented in Table 2.

237 Table 2. CO<sub>2</sub> fluxes and ecological factors of environment for MS 1-4 (median/1 quartile/3  
 238 quartile)  
 239

Parameter	MS 1–4	MS 1	MS 2	MS 3	MS 4
NEE	-103/-152 /-66	-145/-159/- 118	-68/-85/-56	-162/-200/-134	-54/-90/-41
R <sub>eco</sub>	90/74/105	99/86/111	74/67/86	101/79/135	91/85/95
GPP	-200/-251/-151	-237/-266/- 205	-149/-156/-134	-284/-310/-241	-157/-181/- 137
P	218/140/323	291	129	419	144
PAR	1206/1007/136 8	1057/777/140 6	1240/1042/138 7	1217/1100/126 5	1204/1051/1 362
T <sub>air</sub>	31/28/34	31/27/34	32/28/34	32/29/34	32/28/34
T <sub>0</sub>	29/27/37	28/27/38	29/27/37	31/27/38	31/27/37
T <sub>30</sub>	22/22/22	22/22/22	22/22/22	22/22/23	22/22/23
W <sub>0</sub>	22/20/24	21/20/21	23/20/25	22/20/25	22/17/25
W <sub>10</sub>	18/17/19	18/17/21	18/18/23	19/18/19	17/17/18
W <sub>20</sub>	16/15/18	15/13/18	17/15/26	15/13/20	16/16/18
W <sub>30</sub>	13/13/14	13/13/14	15/13/16	13/13/18	13/11/14
W <sub>40</sub>	15/14/16	15/13/16	16/15/16	15/14/16	12/11/14
W <sub>50</sub>	14/13/15	14/13/15	15/15/16	13/13/14	13/12/13
W <sub>60</sub>	14/13/16	14/12/16	16/15/16	15/14/16	12/12/14

W <sub>70</sub>	16/14/17	16/13/18	17/17/18	15/15/18	14/14/14
W <sub>80</sub>	17/17/18	18/13/19	17/17/18	18/15/19	17/16/19
W <sub>90</sub>	19/17/20	17/15/20	17/17/18	22/19/22	20/15/21
W <sub>100</sub>	22/20/24	19/16/20	24/23/24	24/23/26	20/19/22
W <sub>avg</sub>	17/17/18	17/15/17	18/17/19	18/17/18	16/15/17

240 Footnote: the unit for specific CO<sub>2</sub> fluxes (NEE, R<sub>eco</sub>, GPP) is mg C m<sup>-2</sup> h<sup>-1</sup>, for phytomass reserve (P) is g/m<sup>2</sup>,  
241 for temperatures are °C; soil moisture by depth (W<sub>i</sub>) is volumetric moisture – %.  
242

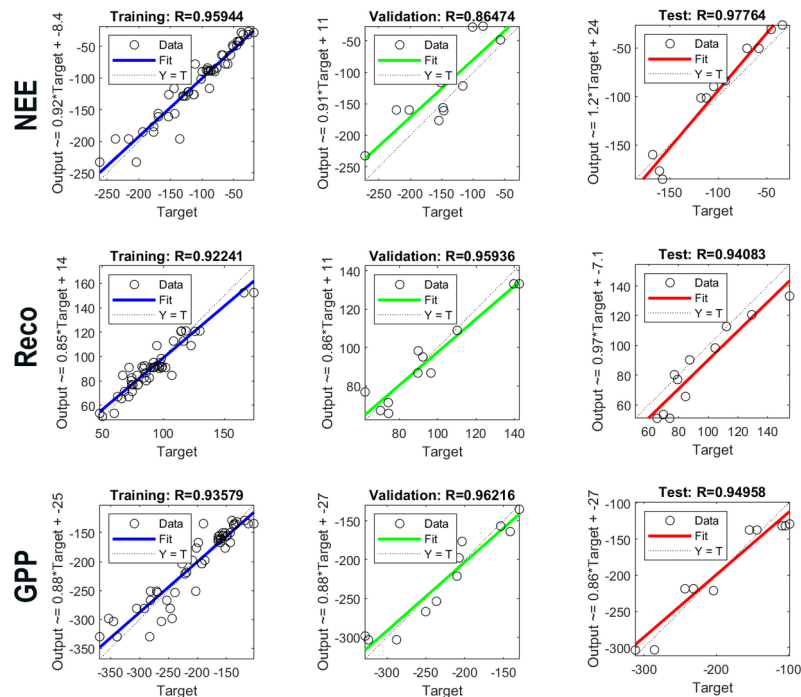
243 To identify significant differences in the magnitude of CO<sub>2</sub> fluxes in the groups between the  
244 MSs, the Kruskal-Wallis test was used at a significance level of  $p=0.01$  (Table 3). The differences  
245 that emerged for NEE and GPP (see Table 3) were most likely associated with the phytomass  
246 reserve (P). Higher values of NEE and GPP for MSs 1 and 3 are associated with higher productivity  
247 values – 291 and 419 g/m<sup>2</sup>, respectively, and lower values of NEE and GPP for MSs 2 and 4 with  
248 lower values – 129 and 144 g/m<sup>2</sup> (see Table 2). We believe that the result of the R<sub>eco</sub> test for MS 4  
249 (see Table 2) is due to moisture reserves in the meter-deep soil layer. A calculation of the moisture  
250 content (average for July 23–25) per 100 cm by MS revealed that MS4 (dominant: *Koeleria*  
251 *pyramidata*) recorded the lowest values – 175 mm. This compares to MS1 (dominant: *Artemisia*  
252 *frigida*) – 181 mm, MS2 (dominants: *Stipa capillata*, *Festuca pseudovina*) – 198 mm, and MS3  
253 (dominant: *Stipa capillata*) – 193 mm. Moreover, comparatively low moisture content was also  
254 observed under MS1, which can be explained by the fact that *Artemisia frigida* is an indicator of  
255 arid conditions (Peat and Bowes, 1994).

256 Table 3. Kruskal-Wallis test for significant differences in CO<sub>2</sub> fluxes in groups between MSs

MS	NEE	R <sub>eco</sub>	GPP
1	A	A	A
2	B	B	B
3	A	A	A
4	B	AB	B

257  
258 An independent estimate of GPP and NPP was obtained using MODIS/Terra satellite data.  
259 According to MOD17A2HGF, for the study area on July 23-28, 2024, GPP values fluctuated  
260 around 310 mg C m<sup>-2</sup> h<sup>-1</sup>, and NPP ~ 230 mg C m<sup>-2</sup> h<sup>-1</sup>. Thus, remote sensing generally agrees well  
261 with the median values for sites 1 and 3, whose plant communities are dominant in the study region.  
262 It should be noted that values of 300–310 mg C m<sup>-2</sup> h<sup>-1</sup> are anomalous and exceed the long-term  
263 average (2000–2024) by 20%, which may be due to high humidity during the study period.  
264 Typically, the maximum in GPP according to MOD17A2HGF was observed in the period June 25 –  
265 July 5, but in 2024 it shifted to July 4 – 12 due to heavy precipitation, leading to an increase in soil  
266 moisture reserves. The GPP reconstruction was based on the hypothesis of a correlation between

267 ground-based instrumental observations of CO<sub>2</sub> fluxes (a short observation series) and variations in  
 268 climatic factors. It was assumed that NN-based methods would allow extrapolation of the obtained  
 269 relationships to a longer time range. To train the NN using cross-correlation, 8 of the 17 measured  
 270 environmental factors were excluded. The exclusion threshold was a correlation coefficient (R)  
 271 greater than 0.5 (in absolute value). As a result, the following predictors were selected for training  
 272 the NN: phytomass reserve (P), air temperature at a height of 100 cm (T<sub>air</sub>), soil temperature at a  
 273 depth of 30 cm (T<sub>30</sub>), soil moisture at depths of 10, 30, 60, 80, 90 cm (W<sub>10</sub>, W<sub>30</sub>, W<sub>60</sub>, W<sub>80</sub>, W<sub>90</sub>). The  
 274 results of NN training for predicting NEE, R<sub>eco</sub>, and GPP fluxes are presented in Figure 2.



275  
 276 Fig. 2. Results of training the NN for predicting the values of NEE, R<sub>eco</sub> and GPP fluxes  
 277 depending on environmental factors: phytomass reserve (P), T<sub>air</sub>, T<sub>30</sub>, W<sub>10</sub>, W<sub>30</sub>, W<sub>60</sub>, W<sub>80</sub>, W<sub>90</sub>. Blue  
 278 – training set, green – validation, red – test  
 279

280 The correlation coefficients for all samples were equal to or greater than 0.9. The resulting NN  
 281 can be used (primarily) for spatial scaling of CO<sub>2</sub> flux values due to the fact that the variability of  
 282 the input parameters during the measurement period was insignificant. The applicability limits of  
 283 the current neural network for the input variables P, T<sub>air</sub>, T<sub>30</sub>, W<sub>10</sub>, W<sub>30</sub>, W<sub>60</sub>, W<sub>80</sub>, W<sub>90</sub> are as follows:  
 284 129–419 g/m<sup>2</sup>, 24–44°C, 21–23°C, 17–23%, 11–18%, 12–16%, 13–19%, 15–22%; accordingly,  
 285 inadequate results may be obtained beyond these limits. With further collection of field data under  
 286 different temporal and environmental conditions, the NN should be further trained. AGP is a key  
 287 parameter in carbon flux studies (Ilyasov et al. 2020). One of the study's hypotheses – to establish a  
 288 link between NEE, R<sub>eco</sub>, and plant community productivity – was also confirmed (see above).

289 Furthermore, our results within the MS range are highly comparable with those for the dry  
290 grasslands of Siberia and Kazakhstan, ranging from 60 to 226 g/m<sup>2</sup> (Titlyanova and Shibareva  
291 2017, p. 50).

292 The good agreement between direct and satellite data in our study of the dry grassland, as well  
293 as in assessing the GPP of extrazonal forest ecosystems in the Altai Krai steppe (Rygalova et al.  
294 2024), strongly suggests further productive work on the temporal and spatial extrapolation of  
295 ground-based data, as well as for the verification and possible calibration of remote sensing data in  
296 the region. It should be noted that progress is currently being made in improving the quality of  
297 remote sensing products, and MODIS data and ground-based measurements are being successfully  
298 used to develop and validate various models for estimating GPP at 10 km resolution (Wang et al.  
299 2024).

300 Various types of NN have demonstrated satisfactory results in predicting GHG emissions,  
301 including backpropagation neural networks (BNNs) and recurrent neural networks (RNNs). These  
302 networks have their own advantages and disadvantages in terms of complexity and the accuracy of  
303 their results (Feng et al. 2024). In our case, a standard two-layer feed-forward neural network  
304 (FNN) was used. A similar example to our study, using a simple NN architecture and a limited set  
305 of input environmental parameters, was obtained in Indonesia for irrigated rice fields when  
306 predicting methane (CH<sub>4</sub>) and nitrogen dioxide (N<sub>2</sub>O). As in our case, air temperature, soil  
307 temperature, and soil moisture were selected as predictors (Chusnul et al. 2025). Clearly, rice fields  
308 have their own specific characteristics, primarily related to soil moisture regimes. However, the use  
309 of soil moisture as a predictor in modeling soil organic carbon content (Luo et al. 2020) and  
310 predicting carbon sinks (Humphrey et al. 2021) is becoming increasingly common. Air  
311 temperature, which we selected as one of the predictors, like atmospheric CO<sub>2</sub> concentration, is a  
312 clear and uncontroversial factor in influencing CO<sub>2</sub> sinks. Closely related to temperature, PAR is  
313 one of the most important factors influencing GPP (Yin et al. 2021). However, in our case, PAR and  
314 temperature were closely correlated, and using both parameters in the model could have introduced  
315 noise. Therefore, given that air temperature is clearly the leading factor, as well as the simple  
316 measurement technology and availability of data, we chose this parameter.

317  
318

## 318 **Conclusions**

319 The work is devoted to measurements of CO<sub>2</sub> fluxes in the dry grassland (true steppe) of the  
320 Altai Krai. Field chamber observations of CO<sub>2</sub> concentration served as the technological basis  
321 for the study. For the first time, estimates of such parameters as net ecosystem exchange,

ecosystem respiration, and gross primary production were obtained for the region. Correlations were revealed between CO<sub>2</sub> fluxes and various environmental factors, such as aboveground phytomass, PAR, air temperature, soil temperature and moisture. The median (1Q, 3Q) NEE, R<sub>eco</sub>, and GPP were, respectively: -103 (-152, -66), 90 (74, 105), and -200 (-251, -151) mg C m<sup>-2</sup> h<sup>-1</sup>. The key factor of variability in NEE and GPP were aboveground phytomass, while for R<sub>eco</sub> was soil moisture content in the 100 cm layer. Based on the obtained data, a neural network was trained using the Levenberg-Marquardt algorithm, which allows for GPP reconstruction using the above-mentioned climatic parameters, where R<sup>2</sup><sub>test</sub> = 0.8.

330

### 331 **References**

332 Al Nuaimi H.S., Acquaye A. and Mayyas A. (2025). Machine learning applications for carbon  
333 emission estimation. *Resources, Conservation & Recycling Advances*, 27, DOI:  
334 10.1016/j.rcradv.2025.200263.

335 Оценка потоков парниковых газов в экосистемах регионов Российской Федерации.  
336 (2023). М.: ИГКЭ, Печать [Assessment of greenhouse gas flows in ecosystems of the regions of  
337 the Russian Federation. (2023). Moscow: IGCE, Print (in Russian)].

338 Система Балочная в Новокормихе (на русском языке). [онлайн] Доступно по адресу:  
339 [https://minprirody-old.alregn.ru/directions/prirodnye\\_resursy/oopt/ooptAK/pamjatniki\\_prirody/  
340 pamjatniki\\_prirody\\_kraevogo\\_znachenija/balochnaja\\_sistema\\_v\\_novokormixe](https://minprirody-old.alregn.ru/directions/prirodnye_resursy/oopt/ooptAK/pamjatniki_prirody/pamjatniki_prirody_kraevogo_znachenija/balochnaja_sistema_v_novokormixe) [Дата  
341 обращения: 30 июня 2025 г.]. [Balochnaya system in Novokormikha [online] Available at:  
342 [https://minprirody-old.alregn.ru/directions/prirodnye\\_resursy/oopt/ooptAK/pamjatniki\\_prirody/  
343 pamjatniki\\_prirody\\_kraevogo\\_znachenija/balochnaja\\_sistema\\_v\\_novokormixe](https://minprirody-old.alregn.ru/directions/prirodnye_resursy/oopt/ooptAK/pamjatniki_prirody/pamjatniki_prirody_kraevogo_znachenija/balochnaja_sistema_v_novokormixe) [Accessed 30 Jun.  
344 2025]. (in Russian)]

345 Beale C.M., Lennon J.J., Yearsley J.M., Brewer M.J. and Elston D.A. (2010). Regression  
346 analysis of spatial data. *Ecol. Lett.*, 13(2), 246-264, DOI: 10.1111/j.1461-0248.2009.01422.x.

347 Belelli Marchesini L., Papale D., Reichstein M., Vuichard N., Tchebakova N. and Valentini R.  
348 (2007). Carbon balance assessment of a natural steppe of southern Siberia by multiple constraint  
349 approach. *Biogeosciences*, 4, 581-595, DOI: 10.5194/bg-4-581-2007.

350 Cenci S. and Biffis E. (2025). Lack of harmonisation of greenhouse gases reporting standards  
351 and the methane emissions gap. *Nat. Commun.*, 16(1), DOI: 10.1038/s41467-025-56845-3.

352 Chusnul A., Purwanto Y.A., Rudiyanto R. and Masaru M. (2025). Neural networks based-  
353 simple estimated model for greenhouse gas emission from irrigated paddy fields. *IAES*

354 *International Journal of Artificial Intelligence (IJ-AI)*, 14, 231-239, DOI:  
355 10.11591/ijai.v14.i1.pp231-239.

356 Cullen L., Marinoni A. and Cullen J. (2024). Machine learning for gap-filling in greenhouse  
357 gas emissions databases. *Journal of Industrial Ecology*, 28(4), 636-647, DOI:  
358 doi.org/10.1111/jiec.13507.

359 Decree of the President of the Russian Federation from November 4, 2020, N 666 “On the  
360 Reduction of Greenhouse Gas Emissions”. (2020). (in Russian). Available at:  
361 <http://publication.pravo.gov.ru/Document/View/0001202011040008> [Accessed 30 May 2025].

362 Dyukarev E.A., Godovnikov E.A., Karpov D.V., Kurakov S.A., Lapshina E.D., Filippov I.V.,  
363 Filippova N.V. and Zarov E.A. (2019). Net Ecosystem Exchange, Gross Primary Production And  
364 Ecosystem Respiration In Ridge-Hollow Complex At Mukhrino Bog. *Geography, Environment,*  
365 *Sustainability*, 12(2), 227-244, DOI: 10.24057/2071-9388-2018-77.

366 Feng W., Chen T., Li L., Zhang L., Deng B., Liu W., Li J. and Cai D. (2024). Application of  
367 Neural Networks on Carbon Emission Prediction: A Systematic Review and Comparison.  
368 *Energies*, 17(7), DOI: 10.3390/en17071628.

369 Ford T.W., Harris E. and Quiring S.M. (2014). Estimating root zone soil moisture using near-  
370 surface observations from SMOS. *Hydrol. Earth Syst. Sci.*, 18(1), 139-154, DOI: 10.5194/hess-18-  
371 139-2014.

372 Gilmanov T.G., Verma S.B., Sims P.L., Meyers T.P., Bradford J.A., Burba G.G. and  
373 Suyker A.E. (2003). Gross primary production and light response parameters of four Southern  
374 Plains ecosystems estimated using long-term CO<sub>2</sub>-flux tower measurements. *Global Biogeochem.*  
375 *Cycles*, 17(2), DOI: 10.1029/2002GB002023.

376 Глаголев М.В. (2010). Аннотированный список литературы по измерениям потоков CH<sub>4</sub>  
377 и CO<sub>2</sub> на болотах России. Динамика окружающей среды и глобальные изменения климата,  
378 1(2), [Glagolev M.V. (2010). Annotated reference list of CH<sub>4</sub> and CO<sub>2</sub> flux measurements from  
379 Russia mires. *Environmental Dynamics and Global Climate Change*, 1(2),  
380 DOI: 10.17816/edgcc121-. (in Russian)]

381 Голубятников Л.Л., Курганова И.Н. и Лопес де Геренью В.О. (2023). Оценка баланса  
382 углерода в степных экосистемах России. Известия Академии наук СССР. Физика атмосферы  
383 и океана [Golubyatnikov L.L., Kurganova I.N. and Lopes de Gerenyu V.O. (2023). Estimation of  
384 Carbon Balance in Steppe Ecosystems of Russia. *Izvestiâ Akademii nauk SSSR. Fizika atmosfery i*  
385 *okeana*, 59(1), 71-87, DOI: 10.31857/S0002351523010042. (in Russian)]

386 Hu Z., Wang G., Sun X., Huang K., Song C., Li Y., Sun S., Sun J. and Lin S. (2024). Energy  
387 partitioning and controlling factors of evapotranspiration in an alpine meadow in the permafrost  
388 region of the Qinghai-Tibet Plateau. *Journal of Plant Ecology*, 17(1), DOI: 10.1093/jpe/rtae002.

389 Humphrey V., Berg A., Ciais P., Gentine P., Jung M., Reichstein M., Seneviratne S.I. and  
390 Frankenberg C. (2021). Soil moisture–atmosphere feedback dominates land carbon uptake  
391 variability. *Nature*, 592, 65-69, DOI: 10.1038/s41586-021-03325-5.

392 Intergovernmental Panel on Climate Change (IPCC). (2023). Climate Change 2022 – Impacts,  
393 Adaptation and Vulnerability: Working Group II Contribution to the Sixth Assessment Report of  
394 the Intergovernmental Panel on Climate Change. Cambridge: Cambridge University Press, DOI:  
395 10.1017/9781009325844.

396 International Plant Names Index (IPNI). [online] Available at: <https://ipni.org> [Accessed 30  
397 May 2025].

398 Kazantsev V.S., Krivenok L.A. and Cherbunina M.Yu. (2018). Methane emissions from  
399 thermokarst lakes in the southern tundra of Western Siberia. *Geography, Environment,  
400 Sustainability*, 11(1), 58-73, DOI: 10.24057/2071-9388-2018-11-1-58-73.

401 Куричева О.А., Максимов А.П., Максимов Т.С., Мамкин В.В., Марунич А.С., Мигловец  
402 М.Н., Михайлов О.А., Панов А.В., Прокушкин А.С., Сиденко Н.В., Шилкин А.В., Лапшина  
403 Е.Д., Курганова И.Н., Авиллов В.К., Варлагин А.В., Гитарский М.Л., Дмитриченко А.А.,  
404 Дюкарев Е.А., Загирова С.В., Замолодчиков Д.Г., Зырянов В.И., Карелин Д.В., Карсанаев  
405 С.В. и Курбатова Ю.А. (2023). RuFlux: Сеть сайтов Eddy Covariance в России. Известия  
406 Российской академии наук. Серия географическая, 87(4), 512-535, DOI:  
407 10.31857/S2587556623040052. [Kuricheva O.A., Maksimov A.P., Maximov T.S., Mamkin V.V.,  
408 Marunich A.S., Miglovets M.N., Mikhailov O.A., Panov A.V., Prokushkin A.S., Sidenko N.V.,  
409 Shilkin A.V., Lapshina E.D., Kurganova I.N., Avilov V.K., Varlagin A.V., Ginarskiy M.L.,  
410 Dmitrichenko A.A., Dyukarev E.A., Zagirova S.V., Zamolodchikov D.G., Zyryanov V.I., Karelin  
411 D.V., Karsanaev S.V. and Kurbatova Y.A. (2023). RuFlux: The Network of the Eddy Covariance  
412 Sites in Russia. *Izvestiâ Rossijskoj akademii nauk. Seriâ geograficheskaâ*, 87(4), 512-535,  
413 DOI: 10.31857/S2587556623040052. (in Russian)]

414 Lavrenko E.M. Steppes of the USSR. (1940). Moscow, Leningrad: Publishing House of the  
415 USSR Academy of Sciences (in Russian).

416 Lavrenko E.M., Karamysheva Z.V. and Nikulina R.I. (1991). Eurasian Steppes. Leningrad:  
417 Nauka. (in Russian)

418 Li J., Gong J., Guldmann J.-M., Li S. and Zhu J. (2020) Carbon Dynamics in the Northeastern  
419 Qinghai–Tibetan Plateau from 1990 to 2030 Using Landsat Land Use/Cover Change Data. *Remote*  
420 *Sens.*, 12(3), DOI: 10.3390/rs12030528.

421 Luo Q., Yang K., Chen Y. and Zhou X. (2020). Method development for estimating soil  
422 organic carbon content in an alpine region using soil moisture data. *Sci. China Earth Sci.*, 63(4),  
423 591-601, DOI: 10.1007/s11430-019-9554-8.

424 Mamkin V.V., Mukhartova Yu.V., Diachenko M.S. and Kurbatova J.A. (2019). Three-Year  
425 Variability Of Energy And Carbon Dioxide Fluxes At Clear-Cut Forest Site In The European  
426 Southern Taiga. *Geography, Environment, Sustainability*, 12(2), 197-212, DOI: 10.24057/2071-  
427 9388-2019-13.

428 Mazzola V., Perks M.P., Smith J., Yeluripati J. and Xenakis G. (2021). Seasonal patterns of  
429 greenhouse gas emissions from a forest-to-bog restored site in northern Scotland: Influence of  
430 microtopography and vegetation on carbon dioxide and methane dynamics. *Eur. J. Soil Sci.*, 72(3),  
431 1332-1353, DOI: 10.1111/ejss.13050.

432 Monitoring greenhouse gas fluxes in natural ecosystems. (2017). Saratov: Amirit (in Russian).

433 Muñoz Sabater J. (2019). ERA5-Land hourly data from 1950 to present. Copernicus Climate  
434 Change Service (C3S) Climate Data Store (CDS). DOI: 10.24381/cds.e2161bac. [online] Available  
435 at: <https://cds.climate.copernicus.eu> [Accessed 10 May 2025].

436 Peat H.C. and Bowes G.G. (1994). Management of Fringed Sagebrush (*Artemisia frigida*) in  
437 Saskatchewan. *Weed Technology*, 8(3), 553-558, DOI: 10.1017/S0890037X00039671.

438 Perez-Quezada J.F., Saliendra N.Z., Akshalov K., Johnson D.A. and Laca E.A. (2010). Land  
439 Use Influences Carbon Fluxes in Northern Kazakhstan. *Rangeland Ecol. Manag.*, 63(1), 82-93,  
440 DOI: 10.2111/08-106.1.

441 Photosynthesis and bioproductivity: methods of determination. (1989). Moscow:  
442 Agropromizdat (in Russian).

443 Pillai N.D., Wille C., Nieberding F., Helbig M. and Sachs T. (2025). Assessing Carbon Flux  
444 Variability in an Alpine Steppe: Insights from Dual-Height Measurements. *EGUsphere* [preprint],  
445 DOI: 10.5194/egusphere-2025-530.

446 Raich J.W. and Potter C.S. (1995). Global patterns of carbon dioxide emission from soils.  
447 *Global Biogeochem. Cycles*, 9(1), 23-36, DOI: 10.1029/94GB02723.

448 Ronginskaya A.V. (1963). Steppes of the southeast of the West Siberian Lowland.  
449 *Transactions of the Central Siberian Botanical Garden*, 6 (in Russian).

450 Running S. and Zhao M. (2021). MODIS/Terra Gross Primary Productivity Gap-Filled 8-Day  
451 L4 Global 500m SIN Grid V061 [Data set]. NASA Land Processes Distributed Active Archive  
452 Center. DOI: 10.5067/MODIS/MOD17A2HGF.061 [Accessed 30 May 2025].

453 Rygalova N.V., Mordvin E.Yu. and Bondarovich A.A. (2024). Productivity and carbon  
454 sequestration of *Pinus sylvestris* L. ribbon forests in the dry steppe of Western Siberia according to  
455 dendrochronology and MODIS satellite measurements. *Contemporary Problems of Ecology*, 6,  
456 975-987, DOI: 10.15372/SEJ20240612.

457 Shokoufeh S., A.A.A.N.A. Suhad and Scholz M. (2021). Impact of climate change on wetland  
458 ecosystems: A critical review of experimental wetlands. *J. Environ. Manag.*, 286,  
459 DOI: 10.1016/j.jenvman.2021.112160.

460 Strategy for the socio-economic development of the Russian Federation with low greenhouse  
461 gas emissions until 2050. (2021). (in Russian). Available at:  
462 <http://static.government.ru/media/files/ADKkCzp3fWO32e2yA0BhtIpyzWfHaiUa.pdf>  
463 [Accessed 30 May 2025].

464 Sukhoveeva O., Karelin D., Lebedeva T., Pochikalov A., Ryzhkov O., Suvorov G. and  
465 Zolotukhin A. (2023). Greenhouse gases fluxes and carbon cycle in agroecosystems under humid  
466 continental climate conditions. *Agriculture, Ecosystems & Environment*, 352,  
467 DOI: 10.1016/j.agee.2023.108502.

468 Titlyanova A.A. and Shibareva S.V. (2017). Phytomass stock and net primary production in  
469 the steppe ecosystems of Siberia and Kazakhstan. *Izvestiya Rossiiskoi Akademii Nauk. Seriya*  
470 *Geograficheskaya*, (4), 43-55, DOI: 10.7868/S0373244417040041. (in Russian)

471 Vuichard N., Ciais P., Beletti L., Smith P. and Valentini R. (2008). Carbon sequestration due to  
472 the abandonment of agriculture in the former USSR since 1990. *Global Biogeochem. Cycles*, 22(4),  
473 DOI: 10.1029/2008GB003212.

474 Wang Y. and Ma Y. (2022). Spatio-temporal patterns of NEE based on upscaling eddy  
475 covariance measurements in the alpine grassland of the Tibetan Plateau. *EGU22-1440*,  
476 DOI: 10.5194/egusphere-egu22-1440.

477 Wang-Erlandsson L., Tobian A., van der Ent R.J., Fetzer I., te Wierik S., Porkka M., Staal A.,  
478 Jaramillo F., Dahlmann H., Singh C., Greve P., Gerten D., Keys P.W., Gleeson T., Cornell S.E.,  
479 Steffen W., Bai X. and Rockström J. (2022). A planetary boundary for green water. *Nat. Rev. Earth*  
480 *Environ.*, 3, 380-392, DOI: 10.1038/s43017-022-00287-8.

481 Wen C., Shan Y., Xing T., Liu L., Yin G., Ye R., Liu X., Chang H., Yi F., Liu S., Zhang P.,  
482 Huang J. and Baoyin T. (2024). Effects of nitrogen and water addition on ecosystem carbon fluxes

483 in a heavily degraded desert steppe. *Global Ecology and Conservation*, 52, DOI:  
484 10.1016/j.gecco.2024.e02981.

485 Yin X., Yue X., Zhou H., Ma Y., Tian C., Cao Y. and Lei Y. (2021). Interannual variability of  
486 gross primary productivity at global FLUXNET sites and its driving factors. *Trans. Atmos. Sci.*,  
487 43(6), 1106-1114, DOI: 10.13878/j.cnki.dqkxxb.20200913001.

488 Zhang W.L., Chen S.P., Chen J., Wei L., Han X.G., Lin G.H. (2007). Biophysical regulations  
489 of carbon fluxes of a steppe and a cultivated cropland in semiarid Inner Mongolia. *Agricultural and*  
490 *Forest Meteorology*, 146, 216-229, DOI: 10.1016/j.agrformet.2007.06.002.

491 Zhukov A.A. and Zhukova E.Yu. (2023). Restored vegetation productivity dynamics at surface  
492 coal mine «Chernogorsky» by satellite data Terra/MODIS. *Lesnoy vestnik / Forestry Bulletin*,  
493 27(2), 96-103, DOI: 10.18698/2542-1468-2023-2-96-103. (in Russian)